Contribution from the Department of Chemistry,
Emory University, Atlanta, Georgia 30322

Costa-Type B_{12} Models: Synthesis, Structural Characterization, and Electrochemistry of Chloro Derivatives

Alessandra Gerli and Luigi G. Marzilli*

Received September 5, 1991

Complexes of the type $[LCo((DO)(DOH)pn)Cl]PF_6$, where (DO)(DOH)pn = $N^2,N^{2'}$-propanediylbis(2,3-butanedione 2-imine 3-oxime) and L = pyridine (py) (**1**), 4-CNpy (**2**), 3-Br-py (**3**), 4-CH_3Opy (**4**), and 4-(Me_2N)py (**5**), and $[(py)_2Co((DO)(DOH)pn)](PF_6)_2$ (**6**) have been synthesized. Compound **1** crystallizes in the monoclinic space group $P2_1/n$ with the following crystallographic parameters: a = 6.913 (4) Å, b = 15.248 (5) Å, c = 21.59 (1) Å, β = 96.28 (5)°, V = 2262 (2), Z = 4, R = 0.055, and R_w = 0.060 for 2875 independent reflections. The axial N-Co-Cl fragment is characterized by Co-N and Co-Cl distances of 1.993 (6) and 2.216 (2) Å. A comparison with the structure of the analogous methyl complex $[pyCo((DO)(DOH)pn)CH_3]PF_6$ (Co-N bond = 2.106 (3) Å) shows that the Co-N(py) distance reflects the σ-donor power of the trans axial ligand. The cyclic voltammogram (CV) of **1** in CH_3CN has a first cathodic peak at -0.44 V vs $Ag/AgNO_3$ (0.01 M) and two subsequent cathodic-anodic peak systems at $E_{1/2}$ = -0.61 V and $E_{1/2}$ = ca. -1.0 V, due to quasi-reversible and reversible charge-transfer processes, respectively. The CVs of **2-4** had profiles similar to that of **1**. As L becomes more basic, the first cathodic peak is shifted cathodically. For **5**, with the very basic 4-(Me_2N)py ligand, the cathodic peak occurred at -0.65 V and overlapped the cathodic/anodic peak system at -0.61 V. However, the cathodic/anodic peak system at -0.61 V was clearly observed for **1-4** and did not shift; it occurred at ca. the same potential as the quasi-reversible Co(III)/Co(II) couple in $Co^{III}((DO)(DOH)pn)Cl_2$ (**7**). The CV of **7** had a reversible Co(II)/Co(I) couple at -1.02 V. The CVs of **1-4** (and probably **5**) provide strong evidence for the presence of **7**, a finding which can be explained by its formation either by a chemical reaction or during the electrochemical process. The ^1H NMR spectra of **1-5** in CD_3CN indicate at most trace amounts of **7**. Therefore, **7** was formed during the reduction process. Probably, the initially electrogenerated $Co^{II}((DO)(DOH)pn)Cl$ attacks the Co(III) starting compound to form **7** and a non-chloro Co(II) derivative. Then, **7** is reduced in the second cathodic wave at -0.61 V. The one-electron reduction of all Co(II) species formed is responsible for the reversible wave at ca. -1.0 V. The Co(II)/Co(I) $E_{1/2}$ values for all the complexes studied are similar to the value reported for base-off aquocobalamin (-1.03 V vs $Ag/AgNO_3$ (0.01 M)).

Introduction

The cyano group in vitamin B_{12}, cyanocobalamin, is introduced during the isolation procedure; the vitamin can be converted in vivo to the active alkylcobalamin coenzymes.[1] These compounds have a neutral heterocyclic N base and an anionic ligand occupying the axial positions. Comparison of the effects of replacing the alkyl ligand with an anionic non-alkyl ligand has played an important role in our understanding of the properties of cobalamins and of simpler model compounds.[2-4] For example, electrochemical[5] and structural studies[6-8] on both alkyl and non-alkyl cobalamins have made possible an assessment of various factors influencing these properties. The electrochemical studies of Savéant and co-workers,[5] for example, have been useful in laying the foundations for understanding the electrochemical behavior of methylcobamide-dependent enzymes (cobamides include cobalamins as a subclass).[9,10]

Cobamides involved in methyl-transfer processes have an interesting dependence on holoenzyme function. For methionine synthase, the Co(II)/Co(I) redox couple is 100 mV more positive than for the free cobalamin.[11] For the corrinoid Fe-S protein of CO dehydrogenase, the Co(II)/Co(I) redox couple is made more positive by dissociation of the axial 5-methoxybenzimidazole, giving the base-off species.[12] This suggests that the biochemical reactivity of such coenzymes may be largely dependent on cobalt redox potential, which in turn may be influenced by axial ligation.

The effect of axial ligation on redox potential is most important for the Co(III)/Co(II) redox process since species involved in the Co(II)/Co(I) redox process have weak, if any, axial ligation. Thus, the Co(II)/Co(I) couple is sensitive primarily to the properties of the equatorial ligand. However, non-alkyl Costa-type derivatives $\{Co((DO)(DOH)pn)X_2$[13] (Figure 1), where (DO)(DOH)pn is the equatorial ligand $N^2,N^{2'}$-propanediylbis(2,3-butanedione 2-imine 3-oxime) and X can be H_2O or halide, and $Co((EMO)(EMOH)pn)X_2$,[14] where the oxime methyl groups in (DO)(DOH)pn are replaced by ethyl groups$\}$ can reproduce the $E_{1/2}$ value for the Co(II)/Co(I) couple in base-off aquocobalamin.[15] Even if this good agreement does not extend to relevant organocobalt species,[14,16] these Costa-type derivatives, which have an equatorial ligand of the same -1 charge and pseudosymmetry as the corrin, appear to be better electrochemical mimics of cobalamins than other B_{12} model systems.[14] For example, cobaloximes, with their dinegative $(DH)_2$ equatorial ligand (DH = monoanion of dimethylglyoxime) have a Co(II)/Co(I) couple at -1.4 V, a value quite different from that of cobalamins.[14] Therefore, it would be interesting to assess the effect of axial ligands on the Co(III)/Co(II) redox process of non-alkyl Costa models, axially ligated by N-donor heterocyclic ligands.

In the past we have established conditions for preparing and crystallizing a great variety of analogous cobalt complexes containing either the $(DH)_2$ or the (DO)(DOH)pn moiety.[7,8,17-20] On

(1) B_{12}; Dolphin, D., Ed.; J. Wiley & Sons: New York, 1982.
(2) Trogler, W. C.; Stewart, R. C.; Epps, L. A.; Marzilli, L. G. *Inorg. Chem.* **1974**, *13*, 1564.
(3) Marzilli, L. G.; Politzer, P.; Trogler, W. C.; Stewart, R. C. *Inorg. Chem.* **1975**, *14*, 2389.
(4) Marzilli, L. G.; Bayo, F.; Summers, M. F.; Thomas, L. B.; Zangrando, E.; Bresciani-Pahor, N.; Mari, M.; Randaccio, L. *J. Am. Chem. Soc.* **1987**, *109*, 6045.
(5) Lexa, D.; Savéant, J. M. *Acc. Chem. Res.* **1983**, *16*, 235.
(6) Rossi, M.; Glusker, J. P.; Randaccio, L.; Summers, M. F.; Toscano, P. J.; Marzilli, L. G. *J. Am. Chem. Soc.* **1985**, *107*, 1729.
(7) Bresciani-Pahor, N.; Forcolin, M.; Marzilli, L. G.; Randaccio; Summers, M. F.; Toscano, P. J. *Coord. Chem. Rev.* **1985**, *63*, 1 and references therein.
(8) Randaccio, L.; Bresciani-Pahor, N.; Zangrando, E.; Marzilli, L. G. *Chem. Soc. Rev.* **1989**, *18*, 225.
(9) Banerjee, R. V.; Harder, S. R.; Ragsdale, S. W.; Matthews, R. G. *Biochemistry* **1990**, *29*, 1129.
(10) Matthews, R. G.; Drummond, J. T. *Chem. Rev.* **1990**, *90*, 1275.
(11) Matthews, R. G.; Banerjee, R. V.; Ragsdale, S. W. *BioFactors* **1990**, *2*, 147.
(12) Ragsdale, S. W.; Lindahl, P. A.; Münck, E. *J. Biol. Chem.* **1987**, *262*, 14289.
(13) Seeber, R.; Parker, W. O., Jr.; Marzilli, P. A.; Marzilli, L. G. *Organometallics* **1989**, *8*, 2377.
(14) Elliott, C. M.; Hershenhart, E.; Finke, R. G.; Smith, B. L. *J. Am. Chem. Soc.* **1981**, *103*, 5558.
(15) $E_{1/2}$(Co(II)/Co(I)) = -0.74 V vs SCE[5] and -0.5 V vs SHE.[11]
(16) Seeber, R.; Marassi, R.; Parker, W. O., Jr.; Kelly, G. *Inorg. Chim. Acta* **1990**, *168*, 127.
(17) Parker, W. O., Jr.; Bresciani-Pahor, N.; Zangrando, E.; Randaccio, L.; Marzilli, L. G. *Inorg. Chem.* **1985**, *24*, 3908.
(18) Parker, W. O., Jr.; Bresciani-Pahor, N.; Zangrando, E.; Randaccio, L.; Marzilli, L. G. *Inorg. Chem.* **1986**, *25*, 1303.

0020-1669/92/1331-1152$03.00/0

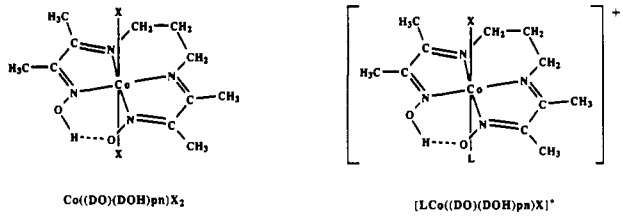

$Co((DO)(DOH)pn)X_2$ $[LCo((DO)(DOH)pn)X]^+$

Figure 1. Structures of non-alkyl (DO)(DOH)pn derivatives.

the basis of a direct comparison of derivatives in the two B_{12} model series, we proposed that the orientation of the planar L ligands is dictated mainly by nonbonded interactions with the equatorial ligands.[17] For example, the cobaloximes invariably have py oriented such that the two α-H atoms are over the six-membered Co–N–O···H–O–N rings. In (DO)(DOH)pn derivatives, steric interaction of the py ligand with the propylene bridge leads to a 90° rotation of the py ligand with respect to the orientation in the cobaloxime series. We suggested that this steric effect, not electronic reasons, could be responsible for the longer Co–N(axial base) bond length and more rapid py dissociation rate observed in (DO)(DOH)pn derivatives when compared to analogous $(DH)_2$ compounds.[17] However, no methods were available to prepare appropriate nonorganometallic Costa-type complexes for comparison with cobaloximes.

In order to determine the possible role that electronic effects may have in influencing the Co–N(axial base) length, we have developed syntheses of (DO)(DOH)pn derivatives containing weak electron-donating ligands trans to the axial base (Figure 1). These compounds make possible an investigation of the dependence of the redox processes on axial ligation. We now report crystallographic data on $[pyCo((DO)(DOH)pn)Cl]PF_6$ (**1**), which contains an axial chloride ligand trans to the axial py ligand. Ligand exchange and cyclic voltammetry studies on this compound and on a series of compounds having different axial ligation, $[4\text{-}CNpyCo((DO)(DOH)pn)Cl]PF_6$ (**2**) (4-CNpy = 4-cyanopyridine), $[3\text{-}Br\text{-}pyCo((DO)(DOH)pn)Cl]PF_6$ (**3**) (3-Br-py = 3-bromopyridine), $[4\text{-}CH_3OpyCo((DO)(DOH)pn)Cl]PF_6$ (**4**) (4-CH_3Opy = 4-methoxypyridine), $[4\text{-}(Me_2N)pyCo((DO)(DOH)pn)Cl]PF_6$ (**5**) (4-(Me_2N)py = 4-(dimethylamino)pyridine), $[(py)_2Co((DO)(DOH)pn)](PF_6)_2$ (**6**), and $Co((DO)(DOH)pn)Cl_2$ (**7**), are also reported. $[pyCo((DO)(DOH)pn)Cl]PF_6$ (**1**) represents the first example of a structurally characterized Costa-type derivative containing a neutral N-donor heterocyclic ligand trans to a weak trans-influencing anionic ligand.

Experimental Section

Reagents. All reagents were from Aldrich except $CoCl_2\cdot 6H_2O$ (Baker) and $(TBA)PF_6$ [$(n\text{-}Bu)_4NPF_6$, Bioanalytical Systems, Inc.]. CH_3CN used in voltammetric experiments was purchased from American Burdick & Jackson (water (%) = 0.004). All other solvents were from Fisher. Elemental analyses were performed by Atlantic Microlabs, Atlanta, GA.

Spectrophotometric Measurements. Visible spectra from 750 to 500 nm were obtained using a matched pair of Teflon-stoppered quartz cells having a path length of 1 cm and a Perkin-Elmer Lambda 3B instrument equipped with a Model 3600 Data Station and thermostated cell compartments (25 ± 0.04 °C). The concentration of the complexes in CH_3CN was 0.01 M.

^{1}H and ^{13}C NMR Spectroscopy. ^{1}H NMR spectra (GE QE-300 spectrometer) were recorded in acetone-d_6 and DMSO-d_6 to assess purity. To interpret the electrochemical results, spectra were also recorded for samples dissolved in CD_3CN in 5-mm tubes with the following parameters: 25° pulse; presaturation of the CHD_2CN; spectral range 6500 Hz; 16K data points; 0.1-Hz line broadening. Reported chemical shifts were based on tetramethylsilane as internal standard. ^{13}C NMR spectra were recorded in CD_3CN. Reported chemical shifts were based in this case on CD_3CN.

Electrochemical Measurements. CVs were recorded with a PAR Model 173 potentiostat equipped with a Model 176 current follower and monitored by a Model 175 universal programmer. The resulting voltammograms were recorded using an Omnigraphic Series 100 X-Y recorder (Houston Instruments). A single-compartment cell with a three-electrode configuration was used. The reference electrode was $Ag/AgNO_3$ (0.01 M) in CH_3CN containing $(TBA)PF_6$ (0.1 M), the counter electrode was a platinum wire, and the working electrode was a platinum disk (BAS MF2013) with a surface area of 0.02 cm^2. The working electrode was polished with fine diamond polish (1-μm particle) before each experiment. Solutions were thoroughly degassed with argon and all voltammetric measurements recorded under a positive pressure of this gas. All determinations were made at least three times, and each voltammetric measurement was carried out using a 10^{-3} M solution of the complex in CH_3CN containing 0.1 M $(TBA)PF_6$. At the end of each voltammetric experiment, bis(cyclopentadienyl)iron(II) was added to the solution. Thus, all potential values could be referred to $E_{1/2}^r$ of this redox couple (Fc^+/Fc), where $E_{1/2}^r$ is an experimental approximation of the standard potential of the redox couple involved, computed as the half-sum of anodic and cathodic peak potentials.[21] In order to allow some comparison with literature data, we point out that, under our experimental conditions, $E_{1/2}^r$ for the couple bis(cyclopentadienyl)iron(III)/iron(II) was +0.09 ± 0.01 V versus $Ag/AgNO_3$. For all the complexes studied, cyclic voltammetric tests were performed at potential scan rates ranging from 0.1 to 0.5 V s^{-1} and at 24 °C.

Preparation of the Complexes. $[pyCo((DO)(DOH)pn)Cl]PF_6$ (1). To a 250-mL Erlenmeyer flask was added $Co((DO)(DOH)pn)Cl_2$[22] (1 g, 2.7 mmol) in 200 mL of aqueous methanol (1:1 v/v), KPF_6 (0.85 g in 20 mL of water), and finally py (0.22 mL, 2.7 mmol). The resulting red solution was filtered through paper in order to remove traces of undissolved material. The flask was left uncovered in the hood at 25 °C. After 4 days, X-ray quality red crystals were collected. (1.1 g, 73% yield). ^{1}H NMR (acetone-d_6): δ 2.61 (6 H, s), 2.80 (6 H, s), 4.38 (4 H, m), 7.45 (2 H, t), 7.97 (3 H, m), 18.92 (1 H, s). Anal. Calcd for $CoC_{16}H_{24}ClF_6N_5O_2P$: C, 34.46; H, 4.34; N, 12.56. Found: C, 34.61; H, 4.35; N, 12.44.

$[4\text{-}CNpyCo((DO)(DOH)pn)Cl]PF_6$ (2) was prepared as above using 4-CNpy (0.28 g, 2.71 mmol). Red crystals formed after the flask was left uncovered in the hood for 1 day; these crystals were collected, rinsed with diethyl ether, and vacuum-dried. (0.62 g, 39% yield). ^{1}H NMR (acetone-d_6): δ 2.60 (6 H, s), 2.80 (6 H, s), 4.39 (4 H, m), 7.82 (2 H, d), 8.34 (2 H, broad signal), 18.89 (1 H, s). Anal. Calcd for $CoC_{17}H_{23}ClF_6N_6O_2P\cdot 2H_2O$: C, 35.01; H, 3.97; N, 14.41. Found: C, 35.04; H, 3.98; N, 14.18.

$[3\text{-}Br\text{-}pyCo((DO)(DOH)pn)Cl]PF_6$ (3) was prepared as above using 3-Br-py (0.43 g, 2.7 mmol). The brown solid that precipitated after 2 h was collected, rinsed with diethyl ether, and vacuum-dried. (0.90 g, 52% yield). ^{1}H NMR (DMSO-d_6): δ 2.58 (6 H, s), 2.71 (6 H, s), 4.01 (4 H, s), 7.36 (1 H, m), 8.02 (1 H, d), 8.52 (1 H, d), 8.67 (1 H, s), 19.10 (1 H, s). Anal. Calcd for $CoC_{16}H_{23}BrClF_6N_5O_2P$: C, 30.19; H, 3.64; N, 11.00. Found: C, 30.26; H, 3.69; N, 10.96.

$[4\text{-}CH_3OpyCo((DO)(DOH)pn)Cl]PF_6$ (4) was prepared as above using 4-CH_3Opy (0.3 g, 2.7 mmol). The brown solid that immediately precipitated was collected, rinsed with diethyl ether, and vacuum-dried. (0.88 g, 55% yield). ^{1}H NMR (acetone-d_6): δ 2.6 (6 H, s), 2.79 (6 H, s), 3.89 (3 H, s), 4.37 (4 H, m), 6.96 (2 H, d), 7.65 (2 H, d), 18.93 (1 H, s). Anal. Calcd for $C_{17}H_{26}CoClF_6N_5O_3P$: C, 34.74; H, 4.46; N, 11.91. Found: C, 34.60; H, 4.45; N, 11.81.

$[4\text{-}(Me_2N)pyCo((DO)(DOH)pn)Cl]PF_6$ (5) was prepared as above using 4-(Me_2N)py (0.33 g, 2.7 mmol) dissolved in 4 mL of methanol. The solution was filtered and left uncovered in the hood. The next day, the solution volume was reduced to ~100 mL with a rotary evaporator (30 °C). The solution was extracted with CH_2Cl_2 (2 × 50 mL portions). Petroleum ether was added to the CH_2Cl_2 layer until the solution became cloudy. The next day, the reddish-brown precipitate formed was collected by vacuum-filtration and rinsed with a small amount of diethyl ether (0.80 g, 49% yield). ^{1}H NMR (acetone-d_6): δ 2.54 (6 H, s), 2.73 (6 H, s), 2.97 (6 H, s), 4.25 (4 H, m), 6.48 (2 H, d), 7.10 (2 H, d). Anal. Calcd for $CoC_{18}H_{29}ClF_6N_6O_2P$: C, 35.98; H, 4.87; N, 13.99. Found: C, 35.90; H, 4.99; N, 13.95.

$[(py)_2Co((DO)(DOH)pn)](PF_6)_2$ (6). To a suspension of $Co((DO)(DOH)pn)Br_2$[22] (1 g, 2.2 mmol) in 100 mL of aqueous methanol (1:1 v/v) was added $AgNO_3$ (0.82 g, 4.4 mmol). The solution was stirred for 0.5 h and then filtered to remove AgBr. Py (0.36 mL, 4.4 mmol) was then added, followed by KPF_6 (0.97 g) in 15 mL of water. The solution was then rotary evaporated until precipitation began. The product was collected by vacuum-filtration and rinsed with a small amount of diethyl ether. The orange solid was recrystallized from acetone/diethyl ether (0.92 g, 53% yield). ^{1}H NMR (acetone-d_6): δ 2.69 (6 H, s), 2.9 (6 H,

(19) Parker, W. O., Jr.; Zangrando, E.; Bresciani-Pahor, N.; Marzilli, P. A.; Randaccio, L.; Marzilli, L. G. *Inorg. Chem.* **1988**, *27*, 2170.
(20) Parker, W. O., Jr.; Bresciani-Pahor, N.; Zangrando, E.; Randaccio, L.; Marzilli, L. G. *Inorg. Chem.* **1986**, *25*, 3489.
(21) Gritzner, G.; Kuta, J. *Pure Appl. Chem.* **1984**, *56*, 461.
(22) Costa, G.; Mestroni, G.; de Savorgnani, E. *Inorg. Chim. Acta* **1969**, *3*, 323.

Table I. Crystallographic Data for [pyCo((DO)(DOH)pn)Cl]PF_6 (**1**)

formula	$CoC_{16}H_{24}ClN_5O_2PF_6$	ρ(calcd), g cm^{-3}	1.63
mol wt	557.741	ρ(measd), g cm^{-3}	1.62
a, Å	6.913 (4)	space group	$P2_1/n$ (No. 14)
b, Å	15.248 (5)	T, °C	25
c, Å	21.59 (1)	λ (Mo Kα), Å	0.71073
β, deg	96.28 (5)	μ, cm^{-1}	9.7
V, Å	2262 (2)	R^a	0.055
Z	4	$R_w{}^b$	0.060

$^a R = \sum||F_o| - |F_c||/\sum|F_o|$. $^b R_w = [\sum||F_o| - |F_c||w^{1/2}/\sum|F_o|w^{1/2}]$.

Table II. Atom Coordinates (×10^4) for [pyCo((DO)(DOH)pn)Cl]PF_6 (**1**)

atom	x	y	z	$10^{-4}U_{equiv}$, Å^2
Co	1155 (1)	2255 (1)	252 (1)	32 (1)^a
Cl	2973 (3)	1073 (1)	463 (1)	45 (1)^a
N(1)	2939 (9)	2875 (4)	812 (3)	42 (2)^a
N(2)	2451 (8)	2405 (4)	−462 (3)	43 (2)^a
N(3)	−559 (8)	1572 (4)	−323 (3)	38 (2)^a
N(4)	−7 (9)	2035 (4)	1005 (3)	39 (2)^a
N(5)	−472 (8)	3320 (4)	58 (3)	40 (2)^a
O(1)	4506 (7)	3275 (3)	624 (3)	55 (2)^a
O(2)	4072 (7)	2893 (3)	−465 (3)	58 (2)^a
C(1)	4101 (14)	3256 (6)	1877 (4)	79 (4)^a
C(2)	2669 (12)	2849 (5)	1392 (4)	50 (3)^a
C(3)	959 (12)	2357 (5)	1499 (4)	49 (3)^a
C(4)	425 (17)	2261 (7)	2143 (4)	84 (4)^a
C(5)	−1795 (11)	1528 (5)	1018 (4)	52 (3)^a
C(6)	−2030 (11)	831 (5)	525 (4)	48 (3)^a
C(7)	−2315 (10)	1187 (5)	−142 (4)	48 (3)^a
C(8)	−1033 (15)	970 (6)	−1388 (4)	78 (4)^a
C(9)	45 (13)	1481 (5)	−869 (4)	52 (3)^a
C(10)	1815 (11)	1964 (5)	−958 (4)	45 (3)^a
C(11)	2774 (16)	1980 (7)	−1539 (4)	81 (4)^a
C(12)	−969 (11)	3859 (4)	498 (4)	46 (3)^a
C(13)	−2075 (12)	4589 (5)	383 (5)	58 (4)^a
C(14)	−2765 (12)	4773 (5)	−228 (5)	60 (4)^a
C(15)	−2266 (12)	4222 (5)	−681 (4)	56 (3)^a
C(16)	−1169 (11)	3517 (5)	−534 (4)	48 (3)^a
P	610 (5)	4652 (2)	7651 (1)	87 (1)^a
F(1a)	−174 (30)	5282 (13)	7152 (9)	145 (6)
F(1b)	−1652 (36)	4600 (15)	7359 (12)	180 (9)
F(2a)	−1511 (39)	4588 (17)	7801 (14)	198 (10)
F(2b)	−254 (35)	3946 (15)	8090 (10)	178 (8)
F(3a)	1213 (30)	4237 (11)	8296 (8)	132 (5)
F(3b)	2680 (43)	4463 (17)	8005 (14)	215 (10)
F(4a)	2672 (26)	4832 (11)	7445 (9)	139 (5)
F(4b)	968 (39)	5000 (16)	6997 (11)	187 (9)
F(5)	667 (25)	5461 (7)	8034 (6)	289 (9)^a
F(6)	637 (18)	3792 (6)	7285 (5)	192 (5)^a

^{a} Equivalent isotropic U defined as one-third of the trace of the orthogonalized U_{ij} tensor.

s), 4.63 (4 H, m), 7.55 (4 H, t), 7.91 (4 H, d), 8.09 (2 H, t). Anal. Calcd for $CoC_{21}H_{29}F_{12}N_6O_2P_2 \cdot {}^3/_4C_3H_6O$: C, 35.35; H, 4.27; N, 10.64. Found: C, 35.35; H, 4.17; N, 10.78.

[(py)$_2$Co(DH)$_2$]PF$_6$. Cobalt(II) nitrate hexahydrate (5.82 g, 0.02 mol) was dissolved in 200 mL of 80% aqueous methanol; the solution was treated with py (14.24 g, 0.18 mol) and then with 4.64 g (0.04 mol) of dimethylglyoxime. The solution was stirred as air was pulled through the solution for 3.5 h. The solution became cloudy and was filtered to remove a fraction of pale pink material, which was discarded. The filtrate was treated with ammonium hexafluorophosphate (3.26 g, 0.02 mol), and the product precipitated as a light gold powder, which was collected and washed with water and methanol; yield 9.74 g (32%). The product was recrystallized from acetone by the addition of water as shiny, dark gold tablets, which were washed with water and methanol and dried in a vacuum desiccator. ^{1}H NMR (DMSO-d_6): δ 2.31 (12 H, s), 7.58 (4 H, t), 8.01 (2 H, t), 8.18 (4 H, d), 18.17 (1 H, s). Anal. Calcd for $CoC_{18}H_{24}F_6N_6O_4P$: C, 36.50; H, 4.08; N, 14.19. Found: C, 36.76; H, 4.10; N, 14.24.

Collection and Reduction of X-ray Data. Crystals of **1** were obtained as described above. Data collection was carried out at ambient temperature on a Nicolet P3F automated four-circle diffractometer equipped with a graphite monochromator. Unit cell parameters were determined on the basis of 25 accurately centered reflections (6° ≤ 2θ ≤ 26°). The

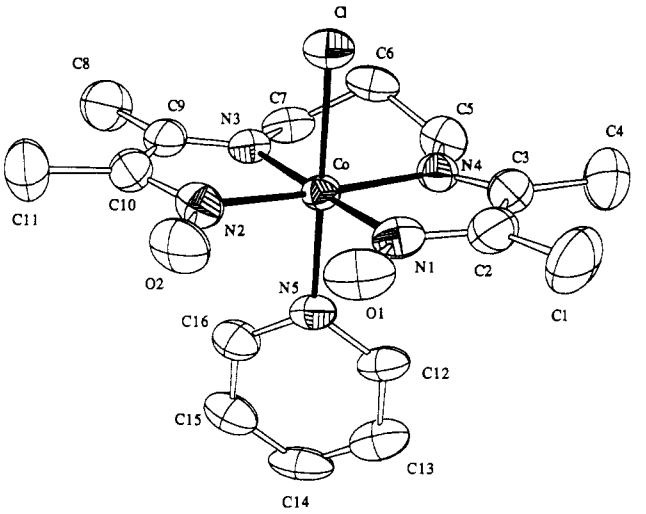

Figure 2. ORTEP drawing (50% probability thermal ellipsoids) and labeling scheme for the non-hydrogen atoms of the cation of [pyCo((DO)(DOH)pn)Cl]PF_6 (**1**).

Table III. Bond Length (Å) with Estimated Standard Deviations for [pyCo((DO)(DOH)pn)Cl]PF_6 (**1**)

Co–N(1)	1.884 (6)	Co–N(4)	1.921 (6)
Co–N(2)	1.880 (6)	Co–N(5)	1.993 (6)
Co–N(3)	1.926 (6)	Co–Cl	2.216 (2)

Table IV. Selected Bond Angles (deg) for [pyCo((DO)(DOH)pn)Cl]PF_6 (**1**)

N(1)–Co–N(2)	97.4 (3)	N(2)–Co–Cl	87.6 (2)
N(1)–Co–N(3)	176.8 (2)	N(3)–Co–N(4)	99.6 (3)
N(1)–Co–N(4)	81.4 (3)	N(3)–Co–N(5)	90.6 (2)
N(1)–Co–N(5)	92.4 (2)	N(3)–Co–Cl	89.3 (2)
N(1)–Co–Cl	87.7 (2)	N(4)–Co–N(5)	92.4 (2)
N(2)–Co–N(3)	81.4 (3)	N(4)–Co–Cl	87.9 (2)
N(2)–Co–N(4)	175.3 (2)	N(5)–Co–Cl	179.7 (1)
N(2)–Co–N(5)	92.1 (2)		

crystal data of interest are given in Table I. Intensities of two standard reflections were measured during data collection and did not show any systematic decay throughout data monitoring. The data were corrected for absorption, by the semiempirical method using Ψ scans, as well for Lorentz and polarization effects.

Structure Solution and Refinement. The structure of **1** was solved by the conventional heavy-atom techniques. The metal atom was located by Patterson syntheses using the program SHELXS-86.[23] Full-matrix least-squares refinement and difference Fourier methods (SHELX-76[24]) were used to locate all remaining non-hydrogen atoms. The atomic scattering factors were taken from a standard source.[25] The PF_6^- anion was found to be disordered. The disorder was interpreted as due to two anion orientations around F(5)-P-F(6) of occupancy 0.5. Hydrogen atoms were included at calculated positions by using a riding model with C–H = 0.96 Å and $U_H = 1.2U_C$. Final R and R_w values are given in Table I. The function minimized was $\sum w(F_o - |F_c|)^2$ where $w = 1/[\sigma^2(F_o) + 0.001F_o^2]$. Final positional parameters are given in Table II. Complete listings of thermal parameters and bond distances and angles are included as supplementary material.

Results

Structural Studies. An ORTEP[26] drawing of the cation of **1** with the atom-labeling scheme is shown in Figure 2. The (DO)(DOH)pn ligand occupies the four equatorial positions of a distorted octahedron around the Co atom. Selected bond lengths and angles are reported in Tables III and IV, respectively. The four equatorial N atoms are coplanar within ±0.0124 (3) Å and

(23) Sheldrick, G. M. SHELXS-86. A Program for Crystal Structure Determination. University of Göttingen, FRG, 1986.
(24) Sheldrick, G. M. SHELX-76. A Program for Crystal Structure Determination. Cambridge University: Cambridge, UK, 1976.
(25) *International Tables for X-ray Crystallography*; Kynoch Press: Birmingham, England, 1974; Vol. IV.
(26) Johnson, C. K. ORTEP. Report ORNL-3794; Oak Ridge National Laboratory: Oak Ridge, TN, 1965.

Table V. ^1H NMR Chemical Shifts (ppm) for **1–7** in CD_3CN[a]

compound	α	β	γ	O—H···O	C—N=C—CH_3	O—N=C—CH_3
[pyCo((DO)(DOH)pn)Cl]PF_6 (**1**)[b]	7.67	7.34	7.85	18.80	2.59	2.50
free py (pK_a = 5.25)[c]	8.57	7.33	7.74			
[4-CNpyCo((DO)(DOH)pn)Cl]PF_6 (**2**)[d]	7.87	7.65	...	18.71	2.60	2.50
free 4-CNpy (pK_a = 1.9)[c]	8.79	7.65	...			
[3-Br-pyCo((DO)(DOH)pn)Cl]PF_6 (**3**)[d]	7.70	7.28	8.03	18.72	2.58	2.49
	7.74					
free-3-Br-py (pK_a = 2.91)[c]	8.68	7.28	7.92			
	8.53					
[4-CH_3OpyCo((DO)(DOH)pn)Cl]PF_6 (**4**)[b]	7.38	6.86	...	18.82	2.60	2.51
free 4-CH_3Opy (pK_a = 6.47)[c]	8.38	6.88	...			
[4-(Me_2N)pyCo((DO)(DOH)pn)Cl]PF_6 (**5**)[b]	6.92	6.42	...	18.86	2.60	2.50
free 4-(Me_2N)py (pK_a = 9.70)[c]	8.12	6.58	...			
[(py)$_2$Co((DO)(DOH)pn)]$(PF_6)_2$ (**6**)[b]	7.53	7.44	7.96	...	2.65	2.52
Co((DO)(DOH)pn)Cl_2 (**7**)[b]	...	...	...	19.40	2.58	2.51
[CH_3CNCo((DO)(DOH)pn)Cl]$^+$[e]	...	...	...	18.82	2.63	2.54

[a] Chemical shifts at 25 °C are relative to internal Me_4Si in CD_3CN. [b] 10^{-3} M solutions. [c] From: Perrin, D. D. *Dissociation Constants of Organic Bases in Aqueous Solution*; Page Bros. Ltd.: Norwich, U.K., 1965. [d] 0.1 M solutions; 6% $CBrCl_3$ added. [e] Signals attributable to this species can be observed in the ^1H NMR spectra of **1–4**.

Table VI. ^1H NMR Chemical Shifts (ppm) of [pyCo((DO)(DOH)pn)X]$^+$ Complexes in CD_3CN[a]

X	α	β	γ	O—H···O	C—N=C—CH_3	O—N=C—CH_3
Cl[b]	7.66	7.36	7.85	18.80	2.60	2.50
CH_3	7.77	7.47	7.93	18.99	2.39	2.29

[a] Chemical shifts at 25 °C are relative to internal Me_4Si, 0.1 M solutions. [b] 6% $CBrCl_3$ added.

the cobalt atom is displaced +0.062 Å from the mean plane toward N(5). The chemically equivalent halves of the equatorial macrocycle with the exclusion of C(6) are approximately planar. These planes exhibit butterfly bending toward the axial chloride ligand and make a dihedral angle, α, of +13.0°. The six-membered chelate has the expected half-chair conformation with the C(6) atom out of the chelate plane on the side of the less bulky chloride. The torsion angles around C(5)–C(6) and C(6)–C(7) bonds are −66.1 and +70.9°, respectively. The O···O distance of the oxime bridge is 2.409 (8) Å.

The Cl–Co–py fragment is characterized by a Cl–Co–N(5) angle of 179.7(1)°. The py residue lies over the five-membered Co–N–C–C–N chelate rings, making a dihedral angle of 88.9° with the equatorial N(1), N(2), N(3), and N(4) coordination plane.

^1H NMR and ^{13}C Spectra. ^1H NMR spectral data of compounds **1–7** (10^{-3} M) were collected in CD_3CN, and relevant chemical shifts of the corresponding pyridine moieties, O–H···O signals, and equatorial methyl signals are reported in Table V. The purpose of these experiments was to determine the extent of pyridine dissociation for **1–6** and the extent of chloride dissociation for **7**, at concentrations used for CV. The axial 4-CNpy in **2** and the 3-Br-py ligand in **3** completely dissociate; only the signals for free 4-CNpy and free 3-Br-py were observed. For [pyCo((DO)(DOH)pn)Cl]PF_6 (**1**) and [4-CH_3OpyCo((DO)(DOH)pn)Cl]PF_6 (**4**), signals corresponding to both free and coordinated pyridine were observed, at ratios of 50:50 and 27:73, respectively. For [4-(Me_2N)pyCo((DO)(DOH)pn)Cl]PF_6 (**5**) there was no evidence for the presence of uncoordinated 4-(Me_2N)py. ^1H NMR data for [(py)$_2$Co((DO)(DOH)pn)]$(PF_6)_2$ (**6**) showed only approximately 3% py dissociation. The ^1H NMR spectrum of **7** shows no evidence for dissociation of chloride. The chemical shifts of free pyridines (10^{-2} M) in CD_3CN are also reported in Table V. ^1H NMR spectra for compounds **2** and **3** (10^{-1} M) in CD_3CN/6% $CBrCl_3$ allowed us to determine the chemical shifts of coordinated 4-CNpy and 3-Br-py (Table V). At high concentrations trace Co(II) impurities lead to line broadening, particularly of the α-H signals. Therefore, $CBrCl_3$, a Co(II) scavenger,[27] was added. ^1H NMR chemical shift data obtained in CD_3CN for [pyCo((DO)(DOH)pn)Cl]PF_6 (**1**) and [pyCo((DO)(DOH)pn)CH_3]PF_6 are compared in Table VI, and ^{13}C chemical shift data in CD_3CN for the same compounds are compared in Table VII.

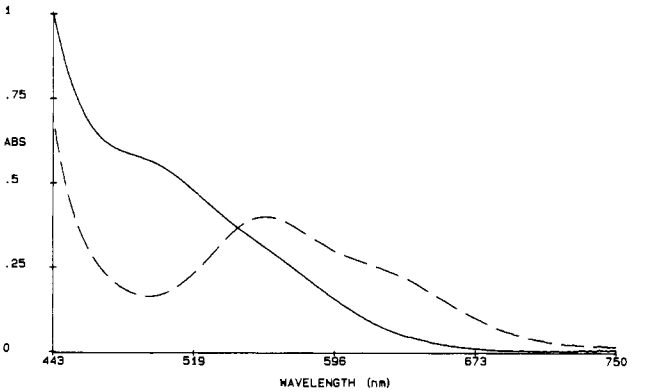

Figure 3. Visible absorption spectra of [pyCo((DO)(DOH)pn)Cl]PF_6 (**1**) (—) and Co((DO)(DOH)pn)Cl_2 (**7**) (– –), 10^{-2} M, in CH_3CN at 25 °C.

Addition of a 20% molar excess of [Ph_4P]Cl to a 10^{-2} M CD_3CN solution of **1** led immediately to full conversion of **1** into **7**. If such a solution of **1** was pretreated with $CBrCl_3$ prior to [Ph_4P]Cl addition, the conversion was retarded and could be followed by ^1H NMR spectroscopy. Under these conditions full conversion to **7** was observed after ~0.5 h. These results are consistent with those obtained by visible spectroscopy.

Visible Spectra. The visible absorption spectra of 10^{-2} M solutions of **1–5** in CH_3CN are relatively featureless, rising steadily toward the UV region (cf. Figure 3). Addition of a 10-fold excess of [Ph_4P]Cl to such a solution of **1** gave a species with the absorption spectrum of **7** immediately. The spectrum of **7** has a clear weak band at 558 nm (ϵ = 41 M^{-1} cm^{-1}). Addition of the Co(II) oxidant $CBrCl_3$ (6%), prior to the addition of [Ph_4P]Cl, retarded the **1** → **7** reaction. The ensuing spectral changes were complex and could not be readily interpreted, perhaps due to the decomposition of $CBrCl_3$ to form HCl. However, a rapid conversion to **7** did not occur. Over the course of ~0.5 h, a spectral band at 558 nm was observed, consistent with formation of **7**.

Cyclic Voltammetric Experiments. The CV of **1** in CH_3CN at 0.2 V/s (Figure 4) had one cathodic peak at −0.44 V and two subsequent cathodic–anodic peak systems at $E_{1/2}$ = −0.61 V and $E_{1/2}$ = −1.01 V due to quasi-reversible and reversible charge-transfer processes, respectively (Table VIII). At higher scan rates, the cathodic peak at −0.44 V shifted cathodically as expected for a reversible charge-transfer process followed by an irreversible chemical reaction.[28]

(27) Marzilli, L. G.; Salerno, J. G.; Epps, L. A. *Inorg. Chem.* **1972**, *11*, 2050.

(28) *Physical Methods of Chemistry, Electrochemical Methods*; Rossiter, B. W., Hamilton, J. F., Eds.; J. Wiley & Sons: New York, 1986; Vol. II.

Table VII. ^{13}C NMR Chemical Shifts (ppm) of $[pyCo((DO)(DOH)pn)X]^+$ Complexes in CD_3CN[a]

X	α	β	γ	C—N=*C	O—N=*C	N*CH$_2$CH$_2$*CH$_2$N	NCH$_2$*CHCH$_2$N	C—N=C—*CH$_3$	O—N=C—*CH$_3$
Cl[b]	150.63	126.72	140.20	179.01	158.16	49.35	27.02	18.07	13.30
CH$_3$	148.24	126.07	138.85	173.89	154.24	49.09	26.79	16.78	12.06

[a] Chemical shifts at 25 °C are relative to Me_4Si, using 117.2 ppm for CD_3CN, 0.1 M solutions. [b] 6% $CBrCl_3$ added.

Table VIII. Cyclic Voltammetric Data for the Reduction of the $Co^{III}(DO)(DOH)pn$ Complexes (10^{-3} M) in CH_3CN Containing 0.1 M $(TBA)PF_6$ at 0.2 V s^{-1} at a Platinum Electrode at 24 °C

complex	Co redox couple	$E_{p,c}$, V	$E_{p,a}$, V	$E_{1/2}$, V	ΔE_p, mV
$[pyCo((DO)(DOH)pn)Cl]PF_6$ (1)	III/II	−0.44			
	III/II	−0.68	−0.53	−0.61	158
	II/I	−1.04	−0.98	−1.01	60
$[4\text{-}CNpyCo((DO)(DOH)pn)Cl]PF_6$ (2)	III/II	−0.39			
	III/II	−0.67	−0.52	−0.60	144
	II/I	−1.03	−0.96	−0.99	70
$[3\text{-}Br\text{-}pyCo((DO)(DOH)pn)Cl]PF_6$ (3)	III/II	−0.39			
	III/II	−0.69	−0.52	−0.61	170
	II/I	−1.06	−0.96	−1.01	100
$[4\text{-}CH_3OpyCo((DO)(DOH)pn)Cl]PF_6$ (4)	III/II	−0.49			
	III/II	−0.67	−0.56	−0.62	110
	II/I	−1.06	−0.98	−1.02	76
$[4\text{-}(Me_2N)pyCo((DO)(DOH)pn)Cl]PF_6$ (5)	III/II	−0.65	−0.50	−0.57	160
	II/I	−1.03	−0.94	−0.99	90
$[(py)_2Co((DO)(DOH)pn)](PF_6)_2$ (6)	III/II	−0.25			
	II/I	−0.99	−0.91	−0.95	76
$Co((DO)(DOH)pn)Cl_2$ (7)	III/II	−0.68	−0.54	−0.61	140
	II/I	−1.06	−0.98	−1.02	76

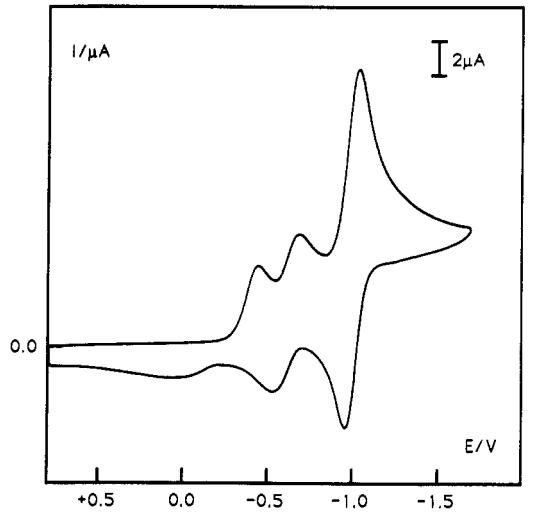

Figure 4. Cyclic voltammogram of $[pyCo((DO)(DOH)pn)Cl]PF_6$ (1) at 0.2 V/s. Potential (E in V) is vs 0.01 M Ag^+/Ag.

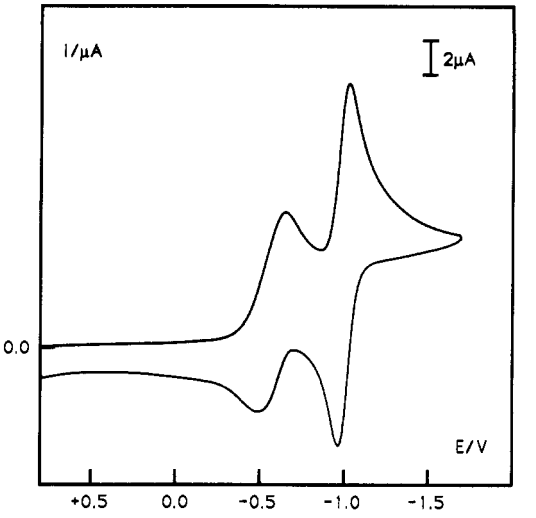

Figure 5. Cyclic voltammogram of $[4\text{-}(Me_2N)pyCo((DO)(DOH)pn)Cl]PF_6$ (5) at 0.2 V/s. Potential (E in V) is vs 0.01 M Ag^+/Ag.

The CVs of **2**, **3**, and **4** at 0.2 V/s showed profiles similar to that of compound **1** (Table VIII). The CV of **5** at 0.2 V/s (Figure 5) had one quasi-reversible wave at −0.57 V and one reversible wave at −0.99 V.

Figure 6 shows the CV of $[(py)_2Co((DO)(DOH)pn)](PF_6)_2$ (**6**). On the direct cathodic scan a first peak was observed at −0.25 V. No anodic peak directly associated with it was observed on the reverse anodic scan at all scan rates attempted (0.1–0.5 V/s). The cathodic–anodic peak system at $E_{1/2}$ = −0.95 V is due to a reversible charge-transfer process.

In an attempt to achieve reversible electrochemical behavior of $[(py)_2Co((DO)(DOH)pn)](PF_6)_2$ (**6**), the CV was recorded in the presence of py (150-fold molar excess). In the presence of py, the first reduction occurred at a more negative potential (−0.46 V) than in its absence. A directly associated peak was observed at −0.06 V in the reverse anodic scan.

The CV of $Co((DO)(DOH)pn)Cl_2$ (**7**) at 0.2 V/s is shown in Figure 7. This complex exhibited two well-defined reduction waves. The first couple at −0.61 V was quasi-reversible, while the more cathodic couple at −1.02 V was reversible.

Upon addition of $[Ph_4P]Cl$ (10-fold molar excess) to a 10^{-3} M CH_3CN solution of **1**, immediate formation of Co((DO)-

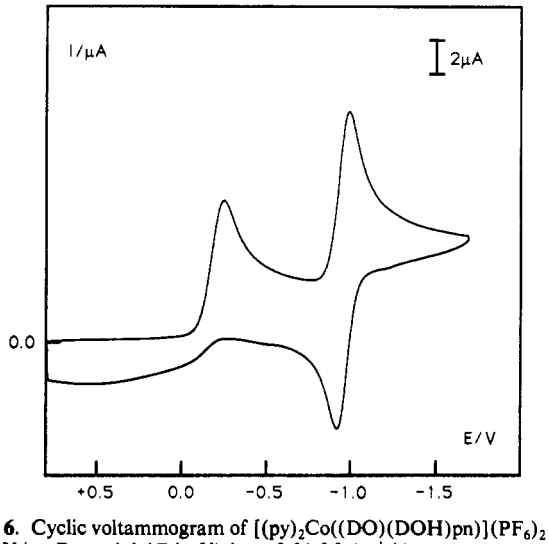

Figure 6. Cyclic voltammogram of $[(py)_2Co((DO)(DOH)pn)](PF_6)_2$ (6) at 0.2 V/s. Potential (E in V) is vs 0.01 M Ag^+/Ag.

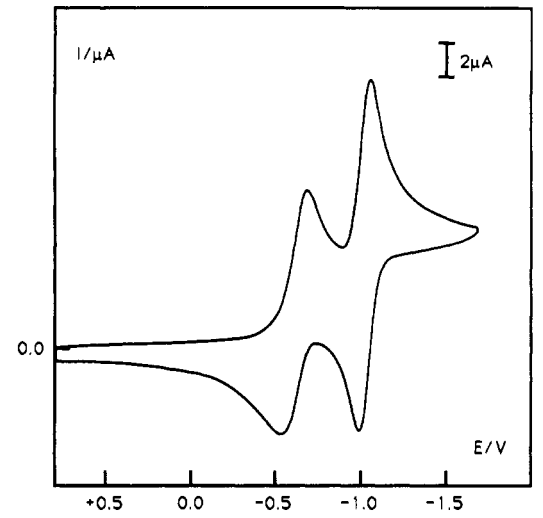

Figure 7. Cyclic voltammogram of Co((DO)(DOH)pn)Cl_2 (**7**) at 0.2 V/s. Potential (E in V) is vs 0.01 M Ag^+/Ag.

(DOH)pn)Cl_2 was observed. The CV recorded for this solution is identical to that for a solution of **7**.

The CV of py$Co(DH)_2Cl$ has one irreversible cathodic wave at −0.90 V, which shifted cathodically with increasing scan rate, and one reversible wave at −1.40 V. A wave due to oxidation of free chloride was also observed at +0.83 V. The CV of $[(py)_2Co(DH)_2]PF_6$ had one irreversible cathodic wave at −0.67 V, which shifted cathodically with increasing scan rate, and one reversible wave at −1.41 V.

Additional Experiments. In order to assess the influence of salt on py dissociation from **1** in CH_3CN, we carried out a few additional voltammetric and ^1H NMR experiments on 10^{-3} M solutions of **1** containing 0.1 M $LiClO_4$. The strong signals of (TBA)PF_6 preclude detection of species at 10^{-3} M in the ^1H NMR spectra. The general electrochemical behavior with $LiClO_4$ was the same as that found with (TBA)PF_6 as a supporting electrolyte. The ^1H NMR spectrum shows the same extent of py dissociation (50%) as in the absence of salt. Therefore, there was no salt effect on py dissociation: the ratio of species in CH_3CN in the absence of salt detected by ^1H NMR spectroscopy reflects the ratio of species present in the (TBA)PF_6-containing CH_3CN solutions that were used to record the CV.

The ^1H NMR O–H···O signal of **6** (10^{-3} M) was too broad to observe, suggesting fast proton exchange. Addition of a 150-fold molar excess of py or 150-fold molar excess of 2-picoline to a 10^{-3} M solution of **6** turned the color of the solution from pale yellow to deep orange. The cyclic voltammetric results for these orange solutions are consistent with deprotonation of the equatorial ligand (vide infra). In order to confirm this hypothesis we carried out a ^1H NMR experiment on a 10^{-3} M solution of **6** to which a 150-fold excess of py-d_5 was added. The equatorial methyl signals in the presence of the excess of py-d_5 move upfield, consistent with deprotonation of the O–H···O group.

Discussion

Structural Comparison. In Table IX some geometrical features of **1** are compared with those for relevant Co(DO)(DOH)pn and $Co(DH)_2$ derivatives. The Co–N(py) distance of 1.993(6) Å in [pyCo((DO)(DOH)pn)Cl]PF_6 is significantly shorter than that of 2.106 (3) Å found in [pyCo((DO)(DOH)pn)CH_3]PF_6.[17] This confirms previous findings that the Co–N(axial base) distance lengthens with the σ-donor power of the trans-axial ligand (electronic trans influence).[7,8]

As has already been observed, another factor that influences the Co–N(axial base) distance is the nature of the equatorial ligand. The Co–N(axial base) distance is longer in [pyCo((DO)(DOH)pn)Cl]PF_6 than in py$Co(DH)_2Cl$.[29] It has been suggested that a significant amount of this Co–N(axial base) lengthening is probably due to a different orientation of the planar N-donor ligand with respect to the equatorial one in the (DO)(DOH)pn analogues.[17] The cobaloximes invariably have the pyridine oriented so that the two α-protons are over the six-membered Co–N–O···H–O–N ring. The substitution of one oxime bridge with a propylene chain in (DO)(DOH)pn derivatives increases the steric interaction between the planar axial base and the nonplanar Co-N-C-C-C-N ring so that an orientation of the py with the α-H protons over the five-membered Co–N–C–C–N ring is favored. This reorientation is presumably also responsible for the increase in butterfly bending in **1** compared to that in py$Co(DH)_2Cl$. Thus the steric clashes are probably more severe in **1** than in organocobalt Costa-type compounds, but these are apparently not so severe as to change the orientation of the py ligand from that found in the organocobalt compounds.

Table IX. Relevant Geometrical Data for (DO)(DOH)pn Complexes and for the Analogous Cobaloximes[a]

axial ligands X	L	Co–X, Å	Co–L, Å	α, deg	d, Å
		(DO)(DOH)pn			
Cl	py[b]	2.216 (6)	1.993 (6)	+13.0	+0.06
CH_3	py[c]	2.003 (3)	2.106 (3)	+6.9	+0.07
		Cobaloximes			
Cl	py[d]	2.229 (1)	1.959 (2)	+0.9	+0.03
CH_3	py[c]	1.998 (5)	2.068 (3)	+3.2	+0.04

[a] Positive values of α and d indicate that the bending of the equatorial ligand is toward X and that the displacement of Co out of the N_4 equatorial donor set is toward L. [b] Present work. [c] Reference 17. [d] Reference 29.

^1H and ^{13}C NMR. A comparison of the α-H shift of the associated pyridine for **1–6** with the α-H shift of the corresponding free pyridine (Table V) shows that on coordination to Co the α-H signal of free pyridine shifts upfield. The α-H signals of the associated pyridines for compounds **1–6** shift upfield as the basicity of the pyridine increases.

There is a linear correlation between these shifts and the corresponding pyridine pK_a values (slope = −0.12, r (linear correlation coefficient) = 0.942). The free pyridines exhibit a similar trend, but a better linear correlation (slope = −0.085, r = 0.981). The poorer correlation for the coordinated pyridines is due to a greater shift upon coordination of the more basic pyridines. The change in the α-H shifts on coordination depends not only on electronic through-bond effects but also on the anisotropy of Co and the equatorial ligand. Although it is difficult to assess the electronic effects, a significant change in Co anisotropy should be reflected in changes in the shifts of the equatorial ligand.[2] However, the methyl signals do not shift very significantly; therefore, Co anisotropy is probably not fully responsible for the changes. Another possibility is that the stronger Co–N(pyridine) bond for the complexes of the more basic pyridines impedes rotations of the pyridine and favors conformers with the α-H over the five-membered ring. Consequently, the α-H's would be influenced more significantly by the equatorial ligand, accounting for the bigger coordination effect on the α-H signal of 4-CH_3Opy and 4-(Me_2N)py.

The O–H···O signals also follow a trend for **1–5**; in particular, a downfield shift is observed for this proton as the basicity of the pyridine increases (slope = 0.021, r = 0.948). The very downfield position of this signal reflects the participation of the H in a strong H-bond. Perhaps the increase in electron donation by the more

(29) Randaccio, L. Personal communication. Other relevant structures with Co–Cl bonds can be found in the following references: Näsäkkälä, M.; Saarinen, H.; Korvenranta, J.; Näsäkkälä, E. *Acta Chem. Scand.* **1979**, *A33*, 431. Siripaisarnpipat, S.; Schlemper, E. O. *J. Coord. Chem.* **1984**, *13*, 281. Choo, P. L.; Mulichak, A. M.; Jones, R. W., Jr.; Bacon, J. W.; Pett, V. B. *Inorg. Chim. Acta* **1990**, *171*, 183. Lopez, C.; Alvarez, S.; Solans, X.; Font-Altaba, M. *Inorg. Chem.* **1986**, *25*, 2962. In some cases, the Co–Cl distances are slightly but significantly longer than that found here.

Scheme I

$$\tfrac{1}{2}[LCo^{III}((DO)(DOH)pn)Cl]^+ + \tfrac{1}{2}e^- \rightarrow \tfrac{1}{2}Co^{II}((DO)(DOH)pn)Cl + \tfrac{1}{2}L$$

$$\tfrac{1}{2}Co^{II}((DO)(DOH)pn)Cl + \tfrac{1}{2}[LCo^{III}((DO)(DOH)pn)Cl]^+ \rightarrow \tfrac{1}{2}Co^{III}((DO)(DOH)pn)Cl_2 + \tfrac{1}{2}[Co^{II}((DO)(DOH)pn)]^+ + \tfrac{1}{2}L$$

$$\tfrac{1}{2}Co^{III}((DO)(DOH)pn)Cl_2 + \tfrac{1}{2}e^- \rightarrow \tfrac{1}{2}[Co^{II}((DO)(DOH)pn)]^+ + Cl^-$$

$$\text{net: } [LCo^{III}((DO)(DOH)pn)Cl]^+ + e^- \rightarrow [Co^{II}((DO)(DOH)pn)]^+ + L + Cl^-$$

basic pyridines leads to better H-bonding and a more downfield shift.

This H-bonding explanation also accounts for the downfield position of the O–H···O signal of [pyCo((DO)(DOH)pn)CH_3]PF_6 compared to the shift for **1**. Electron donation by the axial CH_3 group is expected to be greater than that of the axial chloride (vide infra). The Co anisotropy for **1** is greater than that for [pyCo((DO)(DOH)pn)CH_3]PF_6 (all axial ^{1}H signals are upfield and all equatorial signals are downfield (except O–H···O) in **1**; Table VI).

As mentioned, electronic through-bond effects on ^{1}H shifts are difficult to assess. However, electronic effects are more evident in ^{13}C NMR spectra since, relative to the range of shifts, the Co and ligand anisotropic effects are small. Note that, in every case, the ^{13}C shifts for **1** are downfield from those of [pyCo((DO)(DOH)pn)CH_3]PF_6 (Table VII). This result confirms the expected lower donation by chloride. Thus, a change in anionic axial ligand has a much greater effect on Co anisotropy than a change in axial pyridine ligand basicity.

Ligand Exchange Reactions. Rapidly established substitution equilibria involving a neutral ligand trans to a weak trans-labilizing ligand are rare in Co(III) chemistry. The unexpected behavior of [pyCo((DO)(DOH)pn)Cl]PF_6 (**1**) with added ligand chloride can be explained if this complex, prepared analytically pure by the usual method involving air-oxidation, contains trace Co(II) impurities that catalyze the substitution reaction of py by chloride. Catalysis of the ligand-exchange reaction by the addition of reducing agents is an accepted phenomenon.[27] One of the closest analogies is the reaction of cobaloximes, $LCo(DH)_2X$ (where X = an acido ligand), with neutral monodentate nitrogen or phosphorus donor ligands (L').[27] This reaction yielded $L'Co(DH)_2X$ rather than the expected $[L'Co(DH)_2L]X$. To account for this facile exchange reaction we proposed a mechanism involving an inner-sphere electron transfer via the acido bridge as the rate-limiting step.[27] No exchange occurred when $CBrCl_3$ was added; this result was shown to arise from the oxidation of trace Co(II) impurities. The similarity of these cobaloxime results with those obtained here for the exchange reaction of [pyCo((DO)(DOH)pn)Cl]PF_6 (**1**) with chloride suggests that this substitution is also Co(II) catalyzed. The rapid exchange of py by Cl in the absence of $CBrCl_3$ can be explained by the formation of a chloride bridge between Co(II) and Co(III), followed by atom transfer to form **7**. The system is complex because of the coordinating solvent employed in the present studies.

The same type of mechanism, namely an intermolecular atom transfer, can be invoked to explain the cyclic voltammetric behavior of **1** (vide infra). Here, the electrogenerated Co(II) complex attacks the Co(III) starting compound with formation of a dichloro Co(III) complex and a Co(II) derivative. An outer-sphere electron-transfer mechanism cannot be ruled out, however.

Cyclic Voltammetry. The voltammetric profile of [pyCo((DO)(DOH)pn)Cl]PF_6 (**1**) (Figure 4) is more complicated than the one exhibited typically by non-alkyl mixed-oxime/Schiff-base Co(III) complexes described previously.[13,14] For these compounds, two subsequent cathodic/anodic peak systems corresponding to the reductions Co(III)/Co(II) and Co(II)/Co(I) are generally observed. The Co(II)/Co(I) couple is reversible, is relatively insensitive to the axial ligands, and is mainly influenced by the equatorial chelate. On the other hand, the Co(III)/Co(II) couple depends on the exact axial ligation, shows chemical reversibility, but has a much slower rate of electron transfer than the Co(II)/Co(I) couple. Co((DO)(DOH)pn)Cl_2 (**7**) shows this type of voltammetric profile (Figure 7). The peak systems at $E_{1/2}$ = −0.61 V and $E_{1/2}$ = −1.02 V can be attributed to the couples Co(III)/Co(II) and Co(II)/Co(I), respectively. The neutral complex **7** at 10^{-3} M retains its axial chloride ligands in CD_3CN, as shown by ^{1}H NMR data (Table V). Furthermore, no anodic response attributable to the oxidation of free chloride ions was recorded at ~+1 V vs SCE[30] (or at 0.71 V vs 0.01 M Ag^+/Ag, using the literature[31] value of E = +0.29 V for 0.01 M Ag^+/Ag in CH_3CN vs SCE), and no change in the voltammetric profile was observed upon the addition of chloride ion.

The CV of **1** (Figure 4) has three cathodic peaks: the sum of the peak heights of the first two cathodic peaks is approximately equal to the height of the third peak. If the cathodic peak at −0.44 V is excluded, this voltammetric profile resembles that of compound **7**. In particular, the quasi-reversible couple at −0.61 V occurs at the same potential as the Co(III)/Co(II) couple in compound **7**. This similarity suggests that the reduction of compound **1** proceeds through the mechanism depicted in Scheme I, where $^1/_2$ e^- designates half an equivalent of electrons.

In this generalized scheme, the $Co^{III}Cl$ complex is axially ligated by a combination of neutral ligands (L) which initially is either CH_3CN or a pyridine or an equilibrium mixture of these ligands; the position of equilibrium depends on the pyridine basicity (see below). On reduction, a rapidly equilibrating mixture of five-coordinate Co(II) species is formed with CH_3CN, a pyridine, or chloride as weak axial ligands. Only the latter is depicted in Scheme I because it is the putative species responsible for the formation of the dichloro species (**7**).

Three alternative possibilities were considered to explain the voltammetric profile of **1**: the first two possibilities, that either Cl^- or py in **1** dissociates partially in 10^{-3} M CH_3CN solution, so that two Co(III) species are present initially in solution, would account for the presence of two cathodic peaks at potentials characteristic of a Co(III)/Co(II) redox couple. The third alternate possibility is that a bis(pyridine)cobalt(III) species is formed following reduction of the starting complex.

The first possibility, that chloride dissociates from **1** in 10^{-3} M CH_3CN, could be excluded by the absence of an anodic response due to the oxidation of free chloride ion (Figure 4). For pyCo$(DH)_2$Cl we could observe a wave due to oxidation of free chloride at +0.83 V, in line with Finke's results for (1,5,6-trimethylbenzimidazole)Co$(DH)_2$Cl[14] showing dissociation of the axial chloride in CH_3CN. Thus, the irreversible Co(III)/Co(II) wave at −0.90 V recorded on a 10^{-3} M solution of pyCo$(DH)_2$Cl can be attributed to the reduction of [pyCo$(DH)_2CH_3CN]^+$; the reversible wave at −1.40 V is due to the Co(II)/Co(I) couple.

The CV of [(py)$_2$Co$(DH)_2$]PF_6 has the same Co(II)/Co(I) reversible wave at −1.40 V and also an irreversible peak at −0.67 V attributable to the reduction of $[(py)_2Co^{III}(DH)_2]^+$. The reduction potentials of [(py)$_2$Co$(DH)_2$]PF_6 derived from our voltammetric experiment are similar to the polarographic values reported by Schrauzer for the same compound.[32] However, Schrauzer claimed that pyCo$(DH)_2$Cl and [(py)$_2$Co$(DH)_2$]PF_6 exhibited polarographic waves at the same potentials. We obtained different values.

The second alternate possibility we considered is that the py in **1** dissociates in 10^{-3} M CH_3CN, so that the peaks at −0.44 and −0.61 V are due to the respective reduction of the two species, $[pyCo^{III}((DO)(DOH)pn)Cl]^+$ and $[CH_3CNCo^{III}((DO)(DOH)pn)Cl]^+$, at equilibrium. The ^{1}H NMR spectrum showed that these two species are present in a 50:50 ratio at equilibrium.

(30) Meites, L.; Zuman, P.; Narayanan, A. *Handbook Series in Inorganic Electrochemistry*; 1982; Vol. I, p 248.

(31) Larson, R. C.; Iwamoto, R. T.; Adams, R. N. *Anal. Chim. Acta* **1961**, *25*, 371.

(32) Schrauzer, G. N.; Windgassen, R. J. *J. Am. Chem. Soc.* **1966**, *88*, 3738.

Addition of py will shift the equilibrium toward **1**. However, when py was added to a 10^{-3} M solution of **1** and its concentration systematically increased, the only effect on the CV was a slight cathodic shift of the first cathodic peak. Therefore, we excluded the possibility that the two first cathodic peaks in Figure 4 are due to the respective reduction of two initially present Co(III) species at equilibrium.

A third possibility we considered was electrochemical formation of a bis(pyridine) species, $[(py)_2Co((DO)(DOH)pn)]^{2+}$, instead of the dichloro species **7**. In order to determine whether either of the first two cathodic peaks in Figure 4 was due to the reduction of this dication, we analyzed the voltammetric behavior of a solution prepared with an authentic sample of **6** (Figure 6). On the direct cathodic scan, a peak was observed at −0.25 V. No backward anodic peak directly associated with it was observed at all scan rates attempted (0.1–0.5 V/s). The reversible couple at −0.95 V is readily assigned to the Co(II)/Co(I) couple. The ^1H NMR spectrum of $[(py)_2Co((DO)(DOH)pn)](PF_6)_2$ (**6**) in 10^{-3} M solution does not show evidence of significant uncoordinated py (3%). On the other hand, upon the addition of an excess of py (150-fold molar excess) to a 10^{-3} M CH_3CN solution of compound **6**, the first reduction wave occurs at a more negative potential (−0.46 V) than in the absence of py (Figure 6). An anodic peak directly associated with this first reduction wave is now observed at −0.06 V in the reverse anodic scan. This cathodic shift upon addition of py is probably due to deprotonation of the oxime proton of the equatorial ligand since the same effect was observed upon addition of 2-picoline. This species can act as a base, but it is too bulky to coordinate. In any case, the CV of complex **1** (Figure 4) shows no peak at these potentials. Therefore none of the waves in the CV of **1** (Figure 4) are due to the reduction of a $[(py)_2Co((DO)(DOH)pn)]^{2+}$ species.

At this point, we consider in more detail our original mechanism depicted in Scheme I. In this scheme, the quasi-reversible wave at −0.61 V is due to reduction of $Co((DO)(DOH)pn)Cl_2$ (**7**). This wave has the same scan rate dependence exhibited by the wave recorded on a solution of **7**. We attribute the irreversible cathodic wave at −0.44 V to the reduction of the two species $[pyCo^{III}((DO)(DOH)pn)Cl]^+$ and $[CH_3CNCo^{III}((DO)(DOH)pn)Cl]^+$ in a 50:50 ratio, as shown by ^1H NMR data. Although the current intensities of the first two cathodic peaks in Figure 4 due to reduction of Co(III) species are approximately equal (and total the current intensity of the third peak due to the Co(II)/Co(I) redox couple), this situation is coincidental and also holds for **2**, **3**, and **4** which have different extents of pyridine dissociation.

We excluded involvement of a CE (chemical–electrochemical) mechanism[33] such that only reduction of the more easily reduced species (presumably $[CH_3CNCo^{III}((DO)(DOH)pn)Cl]^+$) is observed. Such a mechanism would imply rapid equilibration in the time scale of the experiment. On the other hand, we know that the rate of interconversion between the two species is slow enough that the resonances of both species at equilibrium are observed by ^1H NMR spectroscopy. Therefore, we considered the possibility that reduction of both species occurs at approximately the same potential. In both cases one-electron reduction leads to formation of one (or more) Co(II) species which attacks the equilibrium mixture of Co(III) complexes with formation of $Co^{III}((DO)(DOH)pn)Cl_2$ (**7**). The one-electron reduction of **7** is responsible for the quasi-reversible wave observed at −0.61 V in Figure 4. The reversible wave at −1.01 V is due to the Co(II)/Co(I) couple.

In order to test this mechanism, we synthesized a series of analogous compounds having pyridines with a large range of pK_a values. ^1H NMR studies demonstrate that the axial py ligands in both $[4\text{-CNpyCo}((DO)(DOH)pn)Cl]PF_6$ (**2**) and $[3\text{-Br-pyCo}((DO)(DOH)pn)Cl]PF_6$ (**3**) dissociate completely in 10^{-3} M CD_3CN solution. Therefore, the cathodic peak at −0.39 V for **2** and **3** corresponds to the Co(III)/Co(II) couple of the fully pyridine-dissociated species, $[CH_3CNCo^{III}((DO)(DOH)pn)Cl]^+$. This peak is ~50 mV less cathodic than the first reduction wave of compound **1** at −0.44 V. We attribute this difference to the contribution of $[pyCo((DO)(DOH)pn)Cl]^+$ to the overall reduction process. The appearance of a second reduction wave for compounds **2** and **3** at −0.60 and −0.61 V, respectively, essentially at the same potential as the Co(III)/Co(II) wave of $Co((DO)(DOH)pn)Cl_2$ (**7**) (Figure 7), demonstrates that the dichloro derivative is formed from $[CH_3CNCo((DO)(DOH)pn)Cl]^+$. For **1–3** there is no evidence of chloride dissociation, as suggested by ^1H NMR data in CD_3CN (10^{-3} M) (Table V), and from the absence of anodic response due to the oxidation of free chloride ion in the CVs of **1–3**.

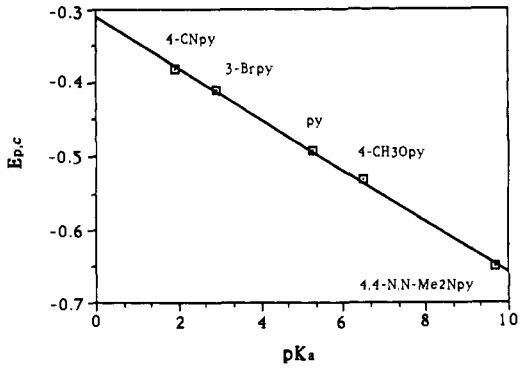

Figure 8. Plot of $E_{p,c}$ of the associated species for **1–5** vs the pK_a values of the corresponding pyridine ligand.

In the case of $[4\text{-}CH_3OpyCo((DO)(DOH)pn)Cl]PF_6$ (**4**), the first cathodic peak at −0.49 V was shifted ~50 mV more cathodic than the same peak in **1** consistent with 4-CH_3Opy being a better electron donor than py. Again, formation of the dichloro species was observed. The size of the second wave indicates that the pyridine-associated species form the dichloro species.

$[4\text{-}(Me_2N)pyCo((DO)(DOH)pn)Cl]PF_6$ (**5**) is the only compound in which the substituted pyridine does not dissociate in 10^{-3} CH_3CN solution. The presence of this excellent electron-donor pyridine shifts the Co(III)/Co(II) reduction potential of $[4\text{-}(Me_2N)pyCo^{III}((DO)(DOH)pn)Cl]^+$ to a much more cathodic value so that the two waves, due to the Co(III)/Co(II) reduction of $[4\text{-}(Me_2N)pyCo((DO)(DOH)pn)Cl]PF_6$ and $Co^{III}((DO)(DOH)pn)Cl_2$, probably merge (Figure 5). As a result, the CV of **5** exhibits only two very well-defined curves; the reversible wave at $E_{1/2} = -0.97$ V is readily assigned to the Co(II)/Co(I) couple.

In the titration of $[pyCo((DO)(DOH)pn)Cl]PF_6$ (**1**) with py, the peak at −0.44 V shifts cathodically (50 mV), consistent with an increase of $[pyCo((DO)(DOH)pn)Cl]PF_6$ at the expense of $[CH_3CNCo((DO)(DOH)pn)Cl]PF_6$ at equilibrium.

The reduction potentials of the nondissociated $[pyCo^{III}((DO)(DOH)pn)Cl]^+$ and $[4\text{-}CH_3OpyCo^{III}((DO)(DOH)pn)Cl]^+$ species could be derived from the percentages of the undissociated forms in 10^{-3} M CD_3CN (NMR) and the potential of the fully dissociated form, $[CH_3CNCo^{III}((DO)(DOH)pn)Cl]^+$ (−0.39 V). The reduction potentials calculated in this way are −0.49 V for $[pyCo^{III}((DO)(DOH)pn)Cl]^+$ and −0.53 V for $[4\text{-}CH_3OpyCo^{III}((DO)(DOH)pn)Cl]^+$. In order to obtain the reduction potentials of the corresponding nondissociated species, we titrated 10^{-3} M solutions of **2** and **3** with increasing amounts of the corresponding pyridine ligand. In the titration of **2** with 4-CNpy we observed that the reduction potential of $[4\text{-CNpy-}Co^{III}((DO)(DOH)pn)Cl]^+$ (−0.38 V) is actually 10 mV more *anodic* than that of the fully dissociated form. Titration of **3** with 3-Br-py indicates that the reduction potential of the associated $[3\text{-Br-py}Co^{III}((DO)(DOH)pn)Cl]^+$ form (−0.41 V) is 20 mV more cathodic than that of the fully dissociated form. In every case for **1–4** the dichloro species is formed, and the relative height of its reduction wave is independent of the pyridine species and independent of addition of excess pyridine. A plot of the reduction potentials of the associated species for compounds **1–5** against the pK_a values of the corresponding pyridine ligand gave a straight

(33) Faure, D.; Lexa, D.; Savéant, J.-M. *J. Electroanal. Chem. Interfacial Electrochem.* **1982**, *140*, 297.

line with slope -0.035 and correlation coefficient of 0.999 (Figure 8). These results demonstrate a marked dependence of the Co(III)/Co(II) cathodic peak on pyridine basicity.

Conclusions

Despite the weaker trans influence of chloride compared to the alkyl group, the py ligand in **1** retains its orientation and increases the butterfly bending. The NMR spectral dependence for Costa-type complexes, now assessed with a non-alkyl complex, has the same trends as found for cobaloximes; namely, the Co anisotropy is greater for the Cl than for the alkyl complexes. Furthermore, the results suggest that the shift of the O-H···O signal depends on axial ligand electronic properties more than on Co anisotropy.

The dichloro complex **7** does not undergo solvolysis in CH_3CN but the pyridine/chloro complexes generally are solvolyzed by loss of pyridine. During electrolytic reduction, the weakly ligated Cl in the electrogenerated Co(II) species is available to convert a second Co(III) species to the dichloro complex. Although this behavior complicates the CV profiles, it was possible to obtain the dependence of the Co(III)/Co(II) peak on pyridine basicity. A 260-mV change in the Co(III)/Co(II) cathodic peak was observed when the axial ligand was changed from 4-CNpy to 4-(Me_2N)py.

No similar systematic study of the redox properties of organocobalt analogues has been done. However, for $[CH_3CNCo((DO)(DOH)pn)CH_3]^+$ and $[CH_3CNCo((DO)(DOH)pn)neo\text{-}C_5H_{11}]^+$ the Co(III)/Co(II) cathodic reduction was found to be -1.42[16] and -1.37 V,[34] respectively, in CH_3CN solvent. The change is ~1.0 V compared to $[CH_3CNCo((DO)(DOH)pn)Cl]^+$. Except for these two alkyl Costa-type complexes, the electrochemical properties of the alkyl Costa-type compounds are complex.

Of some interest, the dimethyl analogue of **7** was observed on reduction of $[CH_3CNCo((DO)(DOH)pn)CH_3]^+$, indicating some unexpected analogy between the alkyl and the non-alkyl species. However, the Co(II) species produced on reduction of $[CH_3CNCo((DO)(DOH)pn)neo\text{-}C_5H_{11}]^+$ is believed to have neopentyl attached to the equatorial ligand.[34] Such species have been recently demonstrated in a related system.[35] The Co(II)/Co(I) cathodic reduction for $[CH_3CNCo((DO)(DOH)pn)neo\text{-}C_5H_{11}]^+$ is -1.4 V, reflecting the change in the equatorial ligand.

Acknowledgment. We are grateful to the National Institutes of Health (Grant GM 29225) for financial support. We also thank Dr. C. L. Hill for the use of the electrochemistry equipment, Dr. P. A. Marzilli for some syntheses, Dr. K. S. Hagen and Dr. M. Sabat for helpful suggestions on the crystallographic study, and Dr. L. Randaccio for communicating unpublished results.

Supplementary Material Available: Tables giving details of the X-ray structural analysis, bond lengths and angles, calculated hydrogen atom coordinates and isotropic thermal parameters, anisotropic thermal parameters, and cyclic voltammetric data for **1-7** at scan rates of 0.1-0.5 V/s and figures showing a crystal packing diagram and CVs at 0.2 V/s of **1** with addition of py, **1** with addition of chloride, **2**, **2** with addition of 4-CNpy, **4**, **6** with addition of py, **6** with addition of 2-picoline, $pyCo(DH)_2Cl$, and $[(py)_2Co(DH)_2]PF_6$ (19 pages); a listing of observed and calculated structure factors (11 pages). Ordering information is given on any current masthead page.

(34) Seeber, R.; Marassi, R.; Parker, W. O., Jr.; Marzilli, L. G. *Organometallics* **1988**, *7*, 1672.

(35) Daikh, B. E.; Finke, R. G. *J. Am. Chem. Soc.* **1991**, *113*, 4160.

Contribution from the Department of Chemistry, University of Tsukuba, Tsukuba, Ibaraki 305, Japan

Synthesis and Properties of Cage-Type S-Bridged $Co^{III}Zn^{II}$ Polynuclear Complexes. Crystal Structure of Spontaneously Resolved $[\{Co(aet)_3\}_4Zn_4O]Br_6$ (aet = 2-Aminoethanethiolate)

Takumi Konno,* Takayuki Nagashio, Ken-ichi Okamoto, and Jinsai Hidaka

Received July 24, 1991

The reaction of *fac*(*S*)-$[Co(aet)_3]$ with $ZnBr_2$ in water produced a cage-type S-bridge polynuclear complex with a "complete" core $[Zn_4O]^{6+}$, $[\{Co(aet)_3\}_4Zn_4O]Br_6$ (**2**), by way of a precursory cage-type complex with a "defective" core $[Zn_3Br]^{5+}$, $[\{Co(aet)_3\}_4Zn_3Br]Br_5$ (**1**). **2** was subject to spontaneous resolution and its crystal structure and absolute configuration for the $(+)_{580}^{CD}$ isomer were determined by X-ray crystallography. $[\{Co(aet)_3\}_4Zn_4O]Br_6 \cdot 9.5H_2O$, chemical formula $C_{24}H_{91}N_{12}O_{10.5}S_{12}Co_4Zn_4Br_6$, crystallizes in the cubic space group $P2_13$ with $a = 18.981$ (1) Å, $V = 6838.6$ (3) Å^3, $Z = 4$, $R = 0.0478$, and $R_w = 0.0448$ for 1844 reflections with $F_o > 5\sigma(F_o)$. The four octahedral *fac*(*S*)-$[Co(aet)_3]$ subunits are bound to the tetrahedral $[Zn_4O]^{6+}$ core in a tetrahedral arrangement, and each Zn(II) is tetrahedrally coordinated by three thiolato sulfur atoms from three different *fac*(*S*)-$[Co(aet)_3]$ subunits and a central μ_4-oxygen atom. For the $(+)_{580}^{CD}$ isomer, chiral configurations are regulated to Λ for all four *fac*(*S*)-$[Co(aet)_3]$ subunits and *R* for all 12 bridging sulfur atoms, giving an approximate T symmetrical structure. Cyclic voltammetric measurements in water exhibited four consecutive quasi-reversible redox couples in the region of -0.3 to -0.9 V (vs Ag/AgCl) for **2**, which correspond to the four Co(III)/Co(II) redox reactions, while **1** exhibited four nonreversible reduction waves in the same potential region. The electronic absorption and circular dichroism (CD) spectral behavior of these complexes are discussed in comparison with those of related mononuclear and linear-type S-bridged trinuclear complexes.

Introduction

One of the most attractive properties of coordinated thiolato ligands is their ability to react readily with a variety of metal ions to form S-bridged polynuclear complexes. For example, a large number of S-bridged polynuclear complexes with 2-aminoethanethiolate (aet, $NH_2CH_2CH_2S^-$) or L-cysteinate (L-cys, $NH_2CH(COO^-)CH_2S^-$) have been prepared using *fac*(*S*)-$[M(aet)_3]$ or *fac*(*S*)-$[M(L\text{-}cys\text{-}N,S)_3]^{3-}$ (M = Co(III), Rh(III), Ir(III)) as the starting complexes.[1-5] It has been recognized that these mononuclear complexes function as tridentate ligands to metal ions such as M' = Fe(III), Co(III), and Ni(II), which prefer

(1) (a) Bush, D. H.; Jicha, D. C. *Inorg. Chem.* **1962**, *1*, 884. (b) Brubaker, G. R.; Douglas, B. E. *Inorg. Chem.* **1967**, *6*, 1562. (c) DeSimone, R. E.; Ontko, T.; Wardman, L.; Blinn, E. L. *Inorg. Chem.* **1975**, *14*, 1313. (d) Blinn, E. L.; Butler, P.; Chapman, K. M.; Harris, S. *Inorg. Chim. Acta* **1977**, *24*, 139. (e) Heeg, M. J.; Blinn, E. L.; Deutsch, E. *Inorg. Chem.* **1985**, *24*, 1118. (f) Johnson, D. W.; Brewer, T. R. *Inorg. Chim. Acta* **1988**, *154*, 221.

0020-1669/92/1331-1160$03.00/0